Preprints.org

Article

Not peer-reviewed version

Anti-HER2 cancer-specific mAb, H2Mab-250-hG$_1$ possesses higher complement-dependent cytotoxicity than trastuzumab

Hiroyuki Suzuki , Tomokazu Ohishi , Tomohiro Tanaka , Mika K. Kaneko , Yukinari Kato *

Posted Date: 11 July 2024

doi: 10.20944/preprints202407.0864.v1

Keywords: HER2; cancer-specific monoclonal antibody; antitumor effect; complement-dependent cellular cytotoxicity

Preprints.org is a free multidiscipline platform providing preprint service that is dedicated to making early versions of research outputs permanently available and citable. Preprints posted at Preprints.org appear in Web of Science, Crossref, Google Scholar, Scilit, Europe PMC.

Copyright: This is an open access article distributed under the Creative Commons Attribution License which permits unrestricted use, distribution, and reproduction in any medium, provided the original work is properly cited.

Preprints.org (www.preprints.org) | NOT PEER-REVIEWED | Posted: 11 July 2024 doi:10.20944/preprints202407.0864.v1

Disclaimer/Publisher's Note: The statements, opinions, and data contained in all publications are solely those of the individual author(s) and contributor(s) and not of MDPI and/or the editor(s). MDPI and/or the editor(s) disclaim responsibility for any injury to people or property resulting from any ideas, methods, instructions, or products referred to in the content.

Article

Anti-HER2 Cancer-Specific mAb, H2Mab-250-hG1 Possesses Higher Complement-Dependent Cytotoxicity than Trastuzumab

Hiroyuki Suzuki [1], Tomokazu Ohishi [2,3], Tomohiro Tanaka [1], Mika K. Kaneko [1] and Yukinari Kato [1,*]

[1] Department of Antibody Drug Development, Tohoku University Graduate School of Medicine, 2-1 Seiryo-machi, Aoba-ku, Sendai, Miyagi 980-8575, Japan; hiroyuki.suzuki.b4@tohoku.ac.jp (H.S.); tomohiro.tanaka.b5@tohoku.ac.jp (T.T.); mika.kaneko.d4@tohoku.ac.jp (M.K.K.)
[2] Institute of Microbial Chemistry (BIKAKEN), Numazu, Microbial Chemistry Research Foundation, 18-24 Miyamoto, Numazu-shi, Shizuoka 410-0301, Japan; ohishit@bikaken.or.jp
[3] Institute of Microbial Chemistry (BIKAKEN), Laboratory of Oncology, Microbial Chemistry Research Foun-dation, 3-14-23 Kamiosaki, Shinagawa-ku, Tokyo 141-0021, Japan
* Correspondence: yukinari.kato.e6@tohoku.ac.jp; Tel.: +81-22-717-8207

Abstract: Cancer-specific monoclonal antibodies (CasMabs) that recognize cancer-specific antigens with *in vivo* antitumor efficacy are innovative therapeutic strategies for minimizing the adverse effects. We previously established a cancer-specific anti-human epidermal growth factor receptor 2 (HER2) monoclonal antibody (mAb), H2Mab-250/H2CasMab-2. In flow cytometry and immunohistochemistry, H2Mab-250 reacted with HER2-positive breast cancer cells but did not show the reactivity to normal epithelial cells. In contrast, a clinically approved anti-HER2 mAb, trastuzumab, strongly recognizes both breast cancer and normal epithelial cells in flow cytometry. The human IgG1 version of H2Mab-250 (H2Mab-250-hG1) possesses compatible *in vivo* antitumor effects against breast cancer xenografts with trastuzumab despite the lower affinity and effector activation than trastuzumab *in vitro*. This study compared the antibody-dependent cellular cytotoxicity (ADCC) and complement-dependent cellular cytotoxicity (CDC) between H2Mab-250-hG1 and trastuzumab. Both H2Mab-250-hG1 and trastuzumab showed ADCC activity against CHO/HER2 and breast cancer cell lines (BT-474 and SK-BR-3) in the presence of human natural killer cells. Some tendency was observed that trastuzumab showed a more significant ADCC effect compared to H2Mab-250-hG1. Importantly, H2Mab-250-hG1 exhibited superior CDC activity in these cells compared to trastuzumab. Similar results were obtained in mouse IgG2a types of both H2Mab-250 and trastuzumab. These results suggest the different contributions of ADCC and CDC activities to the antitumor effects of H2Mab-250-hG1 and trastuzumab and indicate the future direction for the clinical development of H2Mab-250-hG1 against HER2-positive tumors.

Keywords: HER2; cancer-specific monoclonal antibody; antitumor effect; complement-dependent cellular cytotoxicity

1. Introduction

Human epidermal growth factor receptor 2 (HER2) is a member of receptor tyrosine kinases. Heterodimerization of HER2 with other HER family members and the ligands or ligand-independent HER2 homodimerization results in the autophosphorylation of the cytoplasmic domain. The event initiates a variety of signaling, such as RAS-ERK and PI3K-AKT pathways, leading to cancer cell proliferation, survival, and invasiveness [1]. The overexpression of HER2 is observed in

© 2024 by the author(s). Distributed under a Creative Commons CC BY license.

Preprints.org (www.preprints.org) | NOT PEER-REVIEWED | Posted: 11 July 2024 doi:10.20944/preprints202407.0864.v1

approximately 20% of breast cancers [2] and 20% of gastric cancers [3], which are associated with higher rates of recurrence and shorter overall survival.

Trastuzumab, an anti-HER2 monoclonal antibody (mAb), exhibited an *in vitro* anti-proliferative efficacy and a potent antitumor effect *in vivo* [4,5]. The combination of chemotherapy with trastuzumab improves objective response rates, progression-free survival, and overall survival in HER2-positive breast cancer patients with metastasis [6]. Trastuzumab was approved by the U.S. Food and Drug Administration (FDA) for the treatment of HER2-positive breast cancer [6] and has been the most effective therapy for it for more than 20 years [7]. Trastuzumab is administered in patients with HER2-overexpressed tumors, which are defined by solid and complete membranous staining of more than 10% of cells in immunohistochemistry (IHC 3+) and/or *in situ* hybridization (ISH)-amplified [8]. Furthermore, trastuzumab-deruxtecan (T-DXd), a trastuzumab-based antibody-drug conjugate (ADC), has been developed and approved by the FDA [9]. T-DXd exhibited superior efficacy in not only HER2-positive breast cancers [10,11] but also HER2-low (IHC 1+ or IHC 2+ / ISH-non-amplified) advanced breast cancers [12], HER2-mutant lung cancers [13]. Because half of all breast cancers are classifiable as HER2-low, a significant number of patients is estimated to receive the benefit from T-DXd therapy [14].

The immunologic engagement of trastuzumab mediates the clinical efficacy [4]. Antibody-dependent cellular cytotoxicity (ADCC) is elicited by natural killer (NK) cells or macrophages upon the binding of Fcγ receptors (FcγRs) to the Fc region of mAbs [4]. Trastuzumab is a humanized IgG_1 mAb that binds to FcγRs [15] and activates macrophages, dendritic cells, and neutrophils, which change adaptive immune responses by antigen presentation, cytokine production, and chemotaxis [4]. Moreover, the FcγR binding results in the activation of NK cells and macrophages, which can result in the target cell killing [4]. However, the ADCC is impaired by the *N*-linked glycosylation in the Fc region [16]. In particular, a lack of core fucose on the Fc *N*-glycan enhances the Fc binding to the FcγRs on effector cells [17]. Therefore, a core fucose deficiency on the Fc *N*-glycan has been shown to enhance the binding to FcγR on effector cells [17] and exerts potent antitumor effects [18]. The defucosylated recombinant mAbs can be produced using fucosyltransferase 8-knockout Chinese hamster ovary (CHO) cells [19].

The complement-dependent cellular cytotoxicity (CDC) is also exerted by the Fc domain of mAbs [20,21]. Although complements have been thought of as an adjunctive component of the antibody-mediated cytolytic effects, complement is currently considered an essential effector of tumor cytotoxic responses of mAb-based immunotherapy [21]. Through the development of a chimeric anti-CD20 mAb, rituximab, for the treatment of B cell lymphomas, the involvement with the cytolytic capacity of complement was revealed in the antitumor effect [22,23]. In not only anti-CD20 but also anti-CD38 and CD52 immunotherapies, the cytolytic capacity of the tumor by complements has been shown [23–25]. Furthermore, growing pieces of evidence suggest that complement plays crucial functions in not only tumor cytolysis but also several immunologic roles in anti-tumor immunity [26,27]. The crosstalk of complement effectors and cellular signaling pathways influence the T and B cell responses, T helper/effector T cell survival, differentiation, and B cell activation.

A common adverse effect of anti-HER2 mAbs and the ADCs is cardiotoxicity [28]. Routine cardiac monitoring is required for patients [29]. Moreover, the lack of cardiac trabeculae is observed in *ErbB2* (ortholog of *HER2*)-knockout mice [30], and the features of dilated cardiomyopathy are observed in ventricular-specific *ErbB2*-knockout mice [31]. These results indicate that HER2 is involved in normal heart development and homeostasis. Therefore, more selective or specific anti-HER2 mAbs against tumors are required to reduce heart failures.

We previously developed a cancer-specific HER2 mAbs, H_2Mab-214/H_2CasMab-1 [32] and H_2Mab-250/H_2CasMab-2 [33] from 278 clones of anti-HER2 mAbs using glioblastoma LN229-expressed HER2 as an antigen. Notably, both H_2Mab-214 and H_2Mab-250 did not react with spontaneously immortalized normal epithelial cells (HaCaT and MCF 10A) [32,33]. Moreover, H_2Mab-250 did not react with immortalized normal epithelial cells derived from the mammary gland, lung bronchus, gingiva, kidney proximal tubule, thymus, corneal, and colon [33]. In contrast, most anti-HER2 mAbs, including trastuzumab, reacted with both cancer and normal epithelial cells [34].

Preprints.org (www.preprints.org) | NOT PEER-REVIEWED | Posted: 11 July 2024 doi:10.20944/preprints202407.0864.v1

The epitope mapping revealed that the Trp614 in HER2 extracellular domain (ECD) 4 mainly contributes to the recognition by H2Mab-250 [33]. H2Mab-214 also recognized a similar epitope of H2Mab-250, and a crystal structure suggests that H2Mab-214 recognizes a structurally misfolded region in the HER2-ECD4, which usually forms a β-sheet [32]. The result indicates that the local misfolding in the Cys-rich-ECD4 governs the cancer-specificity of H2Mab-214. Furthermore, we produced mouse IgG2a-type and human IgG1-type mAbs from H2Mab-214 and H2Mab-250. We found that both H2Mab-214 and H2Mab-250 possess a compatible *in vivo* antitumor effect against breast cancer xenograft with trastuzumab despite the lower affinity and effector activation than trastuzumab *in vitro* [32,34].

This study compared the ADCC and CDC between H2Mab-250 and trastuzumab against CHO/HER2 and breast cancer cell lines.

2. Results

2.1. ADCC and CDC of H2Mab-250 and Trastuzumab against Breast Cancers

H2Mab-250 recognized HER2-positive breast cancers (BT-474 and SK-BR-3) but did not recognize HER2 in normal epithelial cells. In contrast, trastuzumab recognized both types of HER2 [34]. Because H2Mab-250 and trastuzumab are mouse IgG1 and human IgG1, respectively, we produced human IgG1 type of recombinant H2Mab-250 (H2Mab-250-hG1) and trastuzumab and confirmed the reactivity against breast cancers and normal epithelial cells (Supplementary Figure S1). Although H2Mab-250 possesses ~ 10-fold lower affinity than trastuzumab, H2Mab-250-hG1 possesses compatible antitumor effects against BT-474 and SK-BR-3 xenograft compared to trastuzumab [34]. To reveal the contribution of ADCC and CDC activities to the antitumor effects, we performed *in vitro* ADCC and CDC assay. Both BT-474 and SK-BR-3 cells were labeled with Calcein-AM. Then, calcein release was measured due to the cytotoxicity of mAbs plus human NK cell (ADCC) or mAbs plus complements (CDC). As shown in Figure 1A, both H2Mab-250-hG1 and trastuzumab induced ADCC against BT-474 cells (47% and 64% cytotoxicity, respectively) more effectively than the control human IgG (20% cytotoxicity; $p < 0.01$). Furthermore, trastuzumab showed a superior ADCC compared to H2Mab-250-hG1 ($p < 0.01$). In contrast, H2Mab-250-hG1 showed a significant CDC (47% cytotoxicity) compared to the control human IgG (20% cytotoxicity; $p < 0.05$). However, trastuzumab did not show a significant CDC (Figure 1B). In SK-BR-3, both H2Mab-250-hG1 and trastuzumab induced ADCC (12% and 17% cytotoxicity, respectively) more effectively than the control human IgG (4% cytotoxicity; $p < 0.05$ and $p < 0.01$, respectively, Figure 1C). Moreover, both H2Mab-250-hG1 and trastuzumab exhibited CDC (42% and 26% cytotoxicity, respectively) more effectively than the control human IgG (6% cytotoxicity; $p < 0.01$, Figure 1D). Importantly, H2Mab-250-hG1 showed a superior CDC compared to trastuzumab ($p < 0.01$, Figure 1D). These results suggest the different contributions of ADCC and CDC to the antitumor effects of H2Mab-250-hG1 and trastuzumab.

Preprints.org (www.preprints.org) | NOT PEER-REVIEWED | Posted: 11 July 2024 doi:10.20944/preprints202407.0864.v1

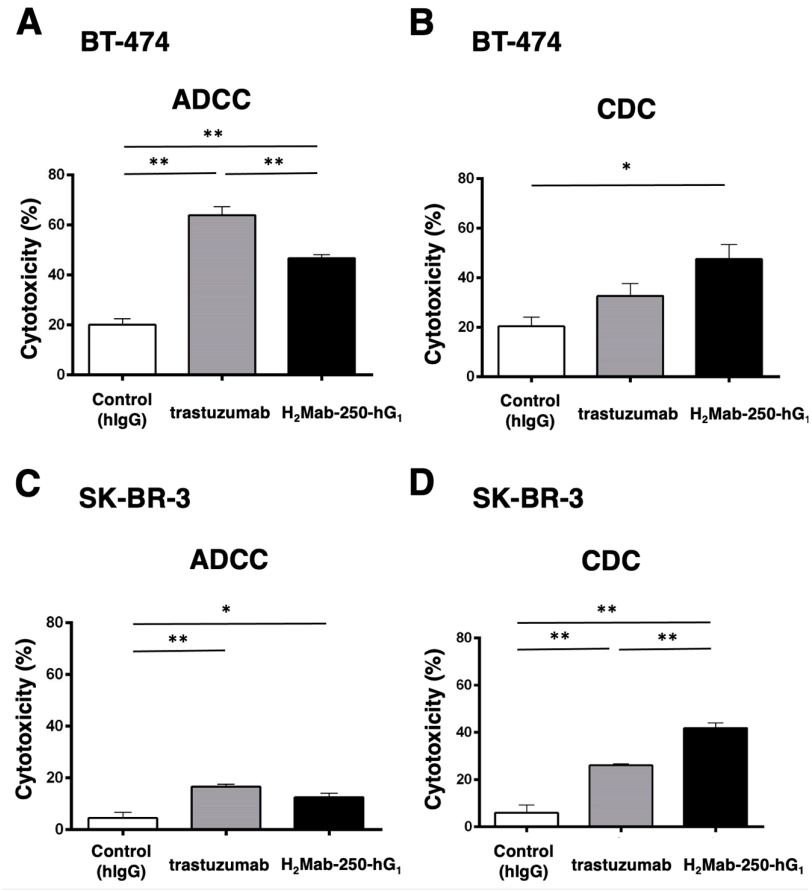

Figure 1. The ADCC and CDC activities were mediated by H2Mab-250-hG1 and trastuzumab in BT-474 and SK-BR-3 cells. (**A**,**C**) The ADCC induced by human NK cells in the presence of H2Mab-250-hG1, trastuzumab, or control human IgG (hIgG) against BT-474 (**A**) and SK-BR-3 (**C**) cells. (**B**,**D**) The CDC induced by complements in the presence of 100 μg/mL of H2Mab-250-hG1, trastuzumab, or control human IgG against BT-474 (**B**) and SK-BR-3 (**D**) cells. Values are shown as the mean ± SEM. Asterisks indicate statistical significance (** $p < 0.01$ and * $p < 0.05$; one-way ANOVA, Tukey's multiple comparisons test).

2.2. ADCC and CDC by H2Mab-250 and Trastuzumab against CHO/HER2

To confirm the requirement of HER2 in ADCC and CDC of H2Mab-250 and trastuzumab, we used CHO-K1 and CHO/HER2 and performed the ADCC and CDC assay. CHO/HER2 was also recognized by H2Mab-250 and trastuzumab with low and high reactivity, respectively [34]. As shown in Figure 2A, both H2Mab-250-hG1 and trastuzumab induced ADCC against CHO/HER2 cells (70% and 77% cytotoxicity, respectively) more effectively than the control human IgG (13% cytotoxicity; $p < 0.01$). In contrast, H2Mab-250-hG1 showed a significant CDC (63% cytotoxicity) compared to the control human IgG (10% cytotoxicity; $p < 0.01$, Figure 2B). However, trastuzumab did not show a significant CDC (Figure 2B). In CHO-K1, we did not observe ADCC and CDC in the presence of H2Mab-250 and trastuzumab (Figure 2C,D). These results indicate that the recognition of HER2 is essential to exert the ADCC and CDC by H2Mab-250-hG1 and trastuzumab. Furthermore, the dose-dependent activation of CDC activity was observed by H2Mab-250 and trastuzumab against CHO/HER2, but not CHO-K1 (Figure 2E). H2Mab-250-hG1 exhibited a significant CDC compared to the control human IgG from 25 μg/mL and showed it compared to trastuzumab at 100 μg/mL (Figure 2E).

Preprints.org (www.preprints.org) | NOT PEER-REVIEWED | Posted: 11 July 2024 doi:10.20944/preprints202407.0864.v1

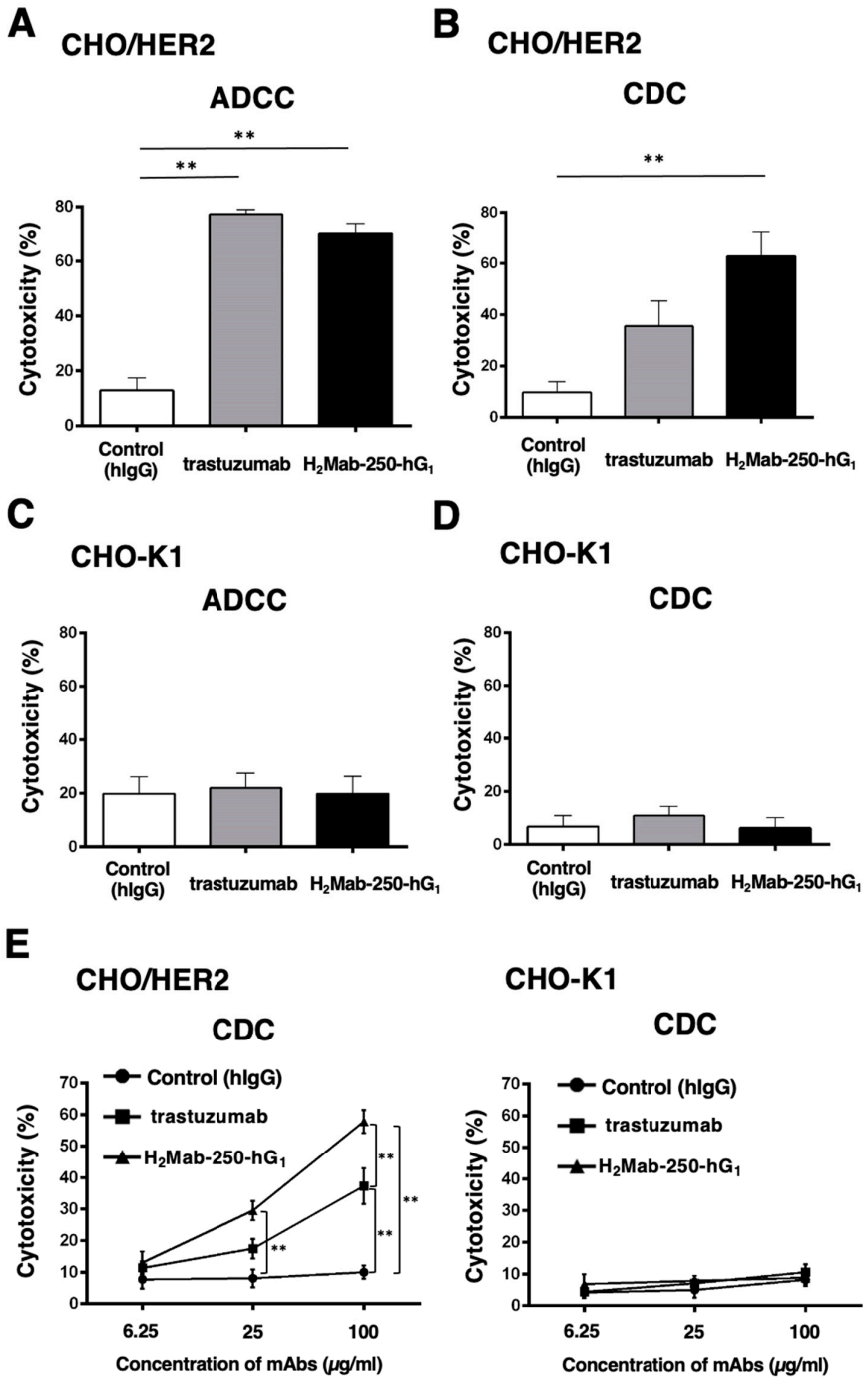

Figure 2. The ADCC and CDC activities are mediated by H_2Mab-250-hG_1 and trastuzumab in CHO/HER2 and CHO-K1 cells. (**A**,**C**) The ADCC induced by human NK cells in the presence of H_2Mab-250-hG_1, trastuzumab, or control human IgG (hIgG) against CHO/HER2 (**A**) and CHO-K1 (**C**) cells. (**B**,**D**) The CDC induced by complements in the presence of 100 μg/mL of H_2Mab-250-hG_1, trastuzumab, or control hIgG against CHO/HER2 (**B**) and CHO-K1 (**D**) cells. Values are shown as the mean ± SEM. Asterisks indicate statistical significance (**$p < 0.01$ and * $p < 0.05$; one-way ANOVA, Tukey's multiple comparisons test). (**E**) The CDC induced by complements in the presence of 6.25, 25, and 100 μg/mL of H_2Mab-250-hG_1, trastuzumab, or hIgG. Values are shown as the mean ± SEM. Asterisks indicate statistical significance (**$p < 0.01$; two-way ANOVA, Tukey's multiple comparisons test).

Preprints.org (www.preprints.org) | NOT PEER-REVIEWED | Posted: 11 July 2024 doi:10.20944/preprints202407.0864.v1

2.3. Antitumor Activities by H₂Mab-250-hG₁ and Trastuzumab

Next, we examined the *in vivo* antitumor efficacy of H₂Mab-250-hG₁ and trastuzumab in the CHO/HER2 xenograft model. We injected H₂Mab-250-hG₁, trastuzumab, and control human IgG intraperitoneally on days 7, 14, and 21 after inoculating CHO/HER2. Furthermore, human NK cells were injected around the tumors on the same days of the Abs injection. Following the inoculation, we measured the tumor volume on days 7, 14, 21, and 28. The H₂Mab-250-hG₁ and trastuzumab administration led to a significant and similar reduction in CHO/HER2 xenograft on day 28 ($p < 0.01$) compared with that of the control (Figure 3A). Both H₂Mab-250-hG₁ and trastuzumab administration resulted in an 81% reduction of CHO/HER2 xenograft volume compared with the control human IgG on day 28.

The CHO/HER2 xenografts from the H₂Mab-250-hG₁- and trastuzumab-treated mice weighed significantly less than those from the control human IgG-treated mice (93 % and 94 % reduction, respectively; $p < 0.05$, Figure 3B,C). There was no significant difference between H₂Mab-250-hG₁- and trastuzumab-treated xenografts.

The body weight loss was not observed in H₂Mab-250-hG₁- and trastuzumab-treated CHO/HER2 xenograft-bearing mice (Figure 3D), and there was no difference in body appearance in those mice (Figure 3E).

We also investigated the pharmacokinetics of H₂Mab-250-hG₁ and trastuzumab after administration in nude mice. As shown in Supplementary Figure S2, the half-life of H₂Mab-250-hG₁ and trastuzumab were determined as 128 and 133 hours, respectively. These results indicated that H₂Mab-250-hG₁ possesses similar half-life compared to trastuzumab.

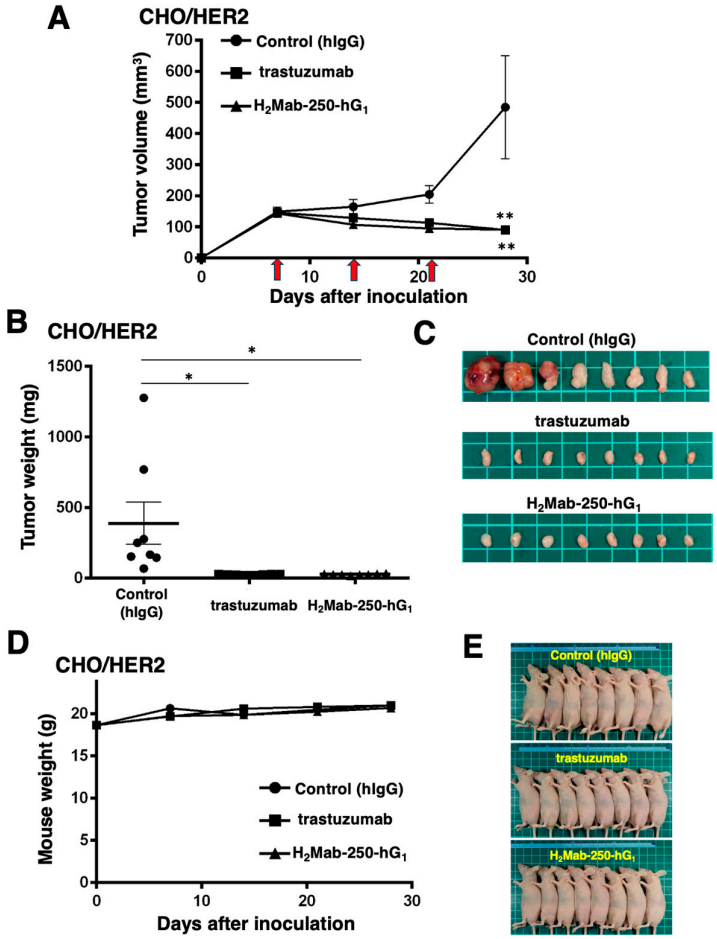

Figure 3. Antitumor activity of H₂Mab-250-hG₁ and trastuzumab against CHO/HER2 xenografts. (**A**) CHO/HER2 cells (5×10^6 cells) were injected subcutaneously into the left flank of BALB/c nude mice (day 0). On day 7, 100 μg of H₂Mab-250-hG₁ (n=8), trastuzumab (n=8), or control human IgG (hIgG)

Preprints.org (www.preprints.org) | NOT PEER-REVIEWED | Posted: 11 July 2024 doi:10.20944/preprints202407.0864.v1

(n=8) were injected into mice. On days 14 and 21, additional antibodies were injected. Human NK cells were injected around the tumors on the same days of Ab administration (arrows). The tumor volume was measured on days 7, 14, 21, and 28. Values are presented as the mean ± SEM. $^{**}p < 0.01$ (two-way ANOVA and Tukey's multiple comparisons test). The tumor weight (**B**) and appearance (**C**) of excised CHO/HER2 xenografts on day 28. Values are presented as the mean ± SEM. $^{*}p < 0.05$ (two-way ANOVA and Tukey's multiple comparisons test). The body weight (**D**) and appearance (**E**) of xenograft-bearing mice treated with trastuzumab, H2Mab-250-hG1, or a control hIgG.

2.4. ADCC and CDC by Mouse IgG2a-type H2Mab-250 and Trastuzumab against CHO/HER2

We next investigate the ADCC and CDC against CHO-K1 and CHO/HER2 using mouse IgG2a-type H2Mab-250 (H2Mab-250-mG2a) and trastuzumab (tras-mG2a) to assess the influence of antibody format. As shown in Figure 4A, tras-mG2a induced ADCC against CHO/HER2 cells (43% cytotoxicity) more effectively than the control mouse IgG2a (10% cytotoxicity; $p < 0.05$). In contrast, H2Mab-250-mG2a did not significantly induce ADCC against CHO/HER2 cells (Figure 4A). Furthermore, both H2Mab-250-mG2a and tras-mG2a induced CDC against CHO/HER2 cells (51% and 45% cytotoxicity, respectively) more effectively than the control mouse IgG2a (Figure 4B, 27% cytotoxicity; $p < 0.05$ and $p < 0.01$, respectively). In CHO-K1, we did not observe ADCC and CDC in the presence of H2Mab-250-mG2a and tras-mG2a (Figure 4C,D).

These results indicate that tras-mG2a showed a superior ADCC compared to H2Mab-250-mG2a. In contrast, H2Mab-250-mG2a exhibited a superior CDC to CHO/HER2 compared to tras-mG2a.

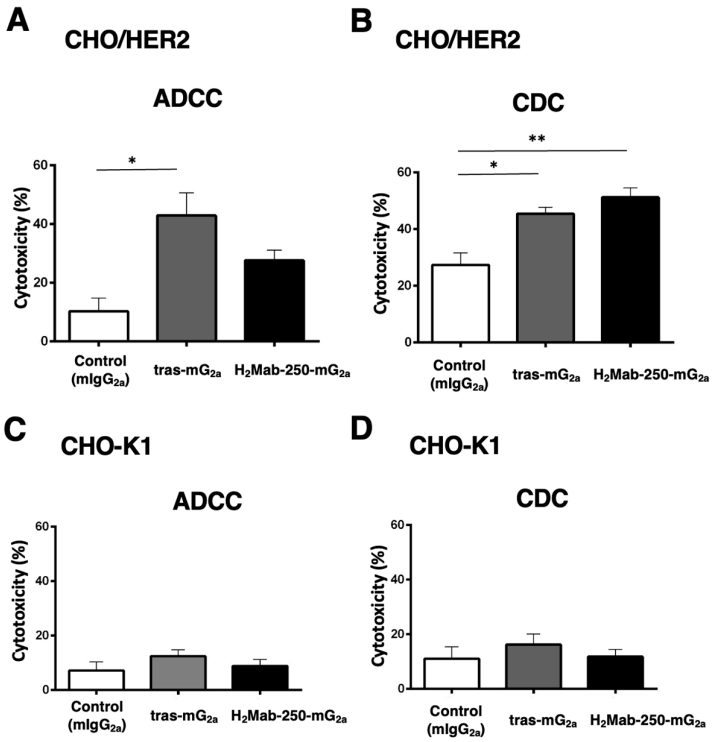

Figure 4. The ADCC and CDC activities are mediated by H2Mab-250-mG2a and tras-mG2a in CHO/HER2 and CHO-K1 cells. (**A**,**C**) The ADCC induced by human NK cells in the presence of 100 μg/mL of H2Mab-250-mG2a, tras-mG2a, or control mouse IgG2a (mIgG2a) against CHO/HER2 (**A**) and CHO-K1 (**C**) cells. (**B**,**D**) The CDC induced by complements in the presence of H2Mab-250-mG2a, tras-mG2a, or control mIgG2a against CHO/HER2 (**B**) and CHO-K1 (**D**) cells. Values are shown as the mean ± SEM. Asterisks indicate statistical significance ($^{**}p < 0.01$ and $^{*}p < 0.05$; one-way ANOVA, Tukey's multiple comparisons test).

Preprints.org (www.preprints.org) | NOT PEER-REVIEWED | Posted: 11 July 2024 doi:10.20944/preprints202407.0864.v1

2.5. Antitumor Activities by Mouse IgG2a-type H2Mab-250 and Trastuzumab

Next, we examined the *in vivo* antitumor efficacy of H2Mab-250-mG2a and tras-mG2a in the CHO/HER2 xenograft model. We injected H2Mab-250-mG2a, tras-mG2a, and a control mouse IgG2a intraperitoneally on days 9 and 16 after inoculating CHO/HER2. Following the inoculation, we measured the tumor volume on days 9, 16, and 21. The H2Mab-250-mG2a and tras-mG2a administration led to a potent and similar reduction in CHO/HER2 xenograft on days 16 and 21 ($p < 0.01$) compared with that of the control mouse IgG2a (Figure 5A). The H2Mab-250-mG2a and tras-mG2a administration resulted in a 77% and 74% reduction of CHO/HER2 xenograft volume compared with the control mouse IgG2a on day 21.

The CHO/HER2 xenografts from the H2Mab-250-mG2a and tras-mG2a-treated mice weighed significantly less than those from the control mouse IgG2a-treated mice (94 % and 94 % reduction, respectively; $p < 0.01$, Figure 5B,C). There is no significant difference between H2Mab-250-mG2a and tras-mG2a-treated xenografts.

Figure 5D shows that body weight loss was not observed in H2Mab-250-mG2a and tras-mG2a-treated CHO/HER2 xenograft-bearing mice. However, a slight difference was observed between control and H2Mab-250-mG2a-treated mice. Those mice have no difference in body appearance (Figure 5E).

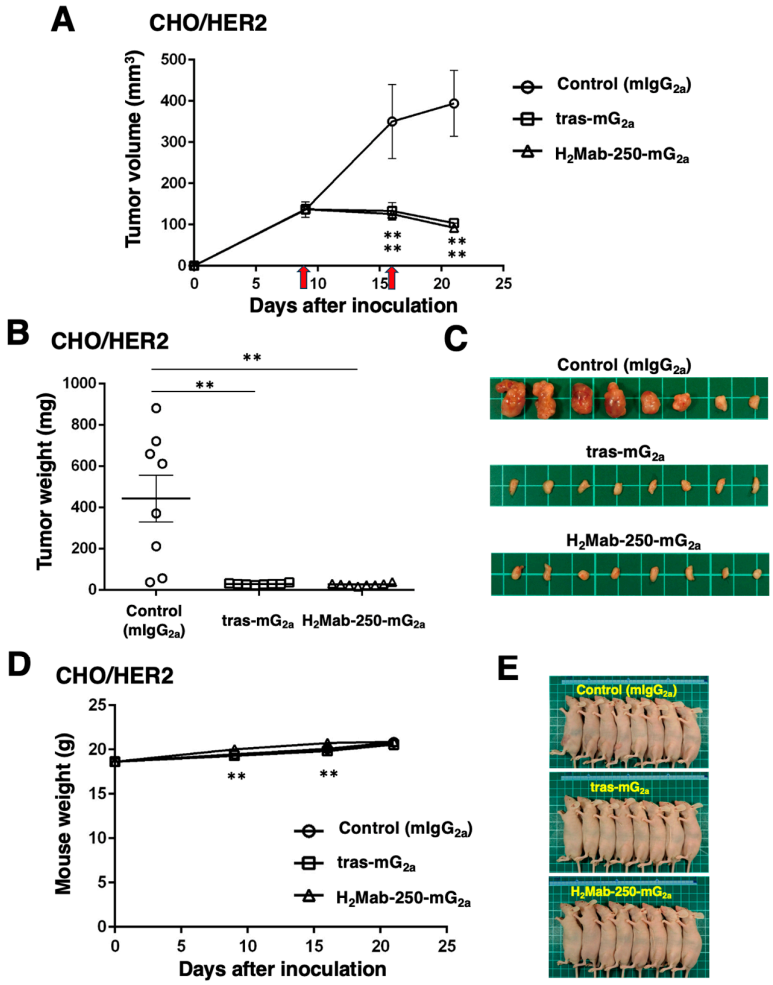

Figure 5. Antitumor activity of H2Mab-250-mG2a and tras-mG2a against CHO/HER2 xenografts. (**A**) CHO/HER2 cells (5×10^6 cells) were injected subcutaneously into the left flank of BALB/c nude mice (day 0). On day 9, 100 μg of H2Mab-250-mG2a (n=8), tras-mG2a (n=8), or a control mouse IgG2a (mIgG2a) (n=8) were injected into mice. On day 16, additional antibodies were injected (arrows). The tumor volume was measured on days 9, 16, and 21. Values are presented as the mean ± SEM. $^{**}p < 0.01$ (two-way ANOVA and Tukey's multiple comparisons test). The tumor weight (**B**) and appearance (**C**) of

Preprints.org (www.preprints.org) | NOT PEER-REVIEWED | Posted: 11 July 2024 doi:10.20944/preprints202407.0864.v1

excised CHO/HER2 xenografts on day 21. Values are presented as the mean ± SEM. *$p < 0.05$ (two-way ANOVA and Tukey's multiple comparisons test). The body weight (**D**) and appearance (**E**) of xenograft-bearing mice treated with H2Mab-250-mG2a and tras-mG2a, or a control mIgG2a.

2.6. Comparison of Antitumor Activities by H2Mab-250-hG1 and Trastuzumab in the Absence of Human NK Cells

As shown in Figure 3, we injected human NK cells with H2Mab-250-hG1 and trastuzumab because high ADCC activity was expected. Since H2Mab-250-hG1 possesses a higher ADCC activity, we next compared the antitumor effects of H2Mab-250-hG1 and trastuzumab without the human NK cells. We injected H2Mab-250-hG1 and trastuzumab intraperitoneally on days 7, 14, and 21 after inoculating CHO/HER2. Following the inoculation, we measured the tumor volume on days 7, 14, 21, and 29. We observed a more potent antitumor efficacy of H2Mab-250-hG1 in both tumor volume ($p < 0.01$, Figure 6A) and weight ($p < 0.01$, Figure 6B) compared with that of trastuzumab at day 29.

Body weight loss was not observed in H2Mab-250-hG1 and trastuzumab-treated CHO/HER2 xenograft-bearing mice (Figure 6D), and there was no difference in body appearance in those mice (Figure 6E).

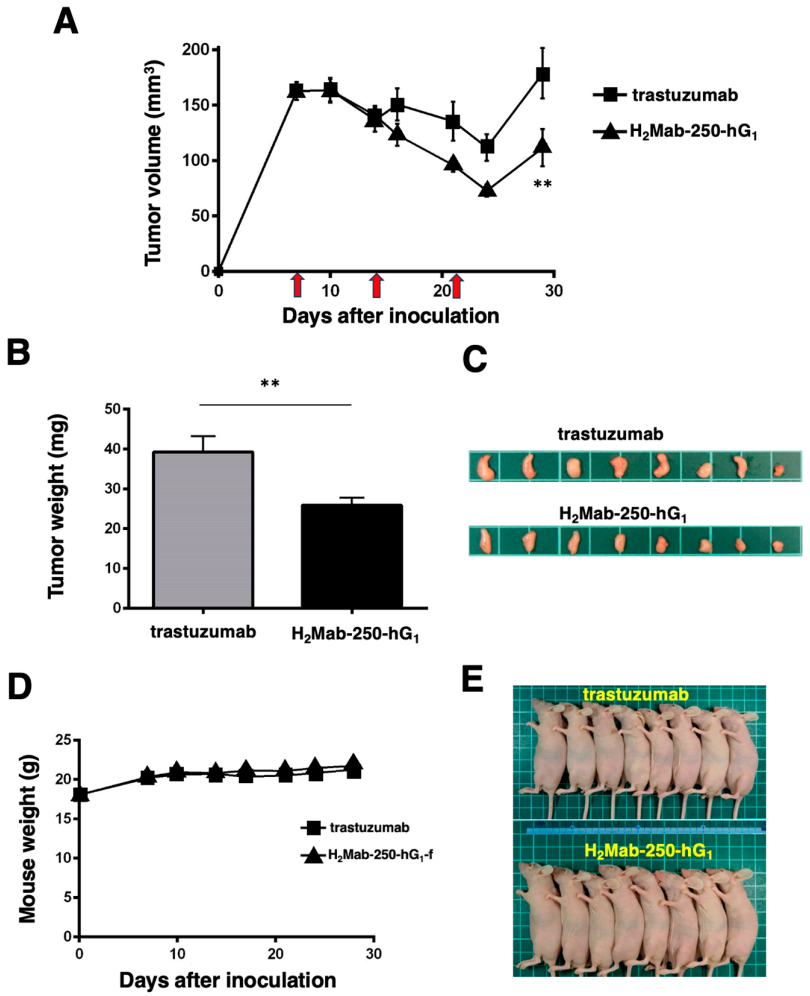

Figure 6. Antitumor activity of H2Mab-250-hG1 and trastuzumab against CHO/HER2 xenografts without human NK cell injection. (**A**) CHO/HER2 cells (5×10^6 cells) were injected subcutaneously into the left flank of BALB/c nude mice (day 0). On day 7, 100 μg of H2Mab-250-hG1 (n=8) or trastuzumab (n=8) were injected into mice. On days 14 and 21, additional antibodies were injected (arrows). The tumor volume was measured on days 7, 10, 14, 16, 21, 24, and 29. Values are presented as the mean ± SEM. **$p < 0.01$ (two-way ANOVA and Tukey's multiple comparisons test). The tumor weight (**B**) and appearance (**C**) of excised CHO/HER2 xenografts on day 29. Values are presented as the mean ± SEM. **$p < 0.01$ (two-way ANOVA

Preprints.org (www.preprints.org) | NOT PEER-REVIEWED | Posted: 11 July 2024 doi:10.20944/preprints202407.0864.v1

and Tukey's multiple comparisons test). The body weight (**D**) and appearance (**E**) of xenograft-bearing mice treated with trastuzumab or H2Mab-250-hG1.

3. Discussion

We have developed CasMabs against HER2 (H2Mab-250 [33,34]), podocalyxin (PcMab-6 [35]), and podoplanin (LpMab-2 [36] and LpMab-23 [37]) by evaluating the reactivity against cancer and normal cells in flow cytometry and immunohistochemistry. We also showed the *in vivo* antitumor effect of the recombinant mAbs (mouse IgG2a or human IgG1 types) derived from the abovementioned mAbs [32–34]. Especially, H2Mab-250 showed a potent antitumor effect *in vivo* [34] despite the lower reactivity and affinity than trastuzumab *in vitro* [33]. However, the reason has not been clarified. In this study, we compared ADCC and CDC activity of H2Mab-250 and trastuzumab and found that H2Mab-250 exhibited a superior CDC activity to breast cancer and HER2-overexpressed cells compared to trastuzumab (Figures 1, 2, and 4). Furthermore, both H2Mab-250-hG1 and H2Mab-250-mG2a showed compatible antitumor effects compared to the corresponding isotype of trastuzumab (Figures 3 and 5). These results suggest that the CDC activity of H2Mab-250 would compensate for the lower ADCC activity in the antitumor efficacy.

Complement is an essential effector of tumor cytotoxic responses in mAb-based immunotherapy [21]. The engagement of the Fc domain of mAbs with complement C1q triggers the assembly of the active C1 complex (C1q, C1r, and C1s), which initiates the cascade. The downstream activation of terminal complement components results in the assembly of the pore-forming membrane attack complex (MAC or C5b–C9) on the tumor cell membrane, which promotes the terminal lytic pathway [21]. Complement activation also leads to tumor cell opsonization by C3-derived opsonins (C3b, iC3b, and C3dg), which bind to CR3 / CR4 complement receptors on phagocytes (neutrophils and macrophages) and augment the FcγR-dependent phagocytic uptake of opsonized tumor cells. Furthermore, complement activation generates pro-inflammatory mediators (C3a and C5a). The anaphylatoxin C5a upregulates FcγRs on phagocytes and primes them for enhanced phagocytosis and increasing the magnitude of the tumor cytolytic response [21].

Because H2Mab-250 showed increased CDC activity only in the presence of complement (Figures 1, 2, and 4), the assembly of MAC is thought to be efficiently formed on the cells. Furthermore, the predisposition to CDC of H2Mab-250 is independent of the isotype or species of mAbs (Figures 2 and 4). Therefore, the complementarity-determining region and epitope of H2Mab-250 are thought to be necessary. In Figure 6, the antitumor effects of H2Mab-250-hG1 were higher than that of trastuzumab without human NK cells, indicating that H2Mab-250-hG1 exerts antitumor activities with much higher CDC than trastuzumab *in vivo*. Several factors, including antigen size and density, determine the engagement of the classical complement pathway. In addition, a geometry of the antigen-mAb complex allows efficient C1q binding [38]. Further investigation and confirmation are required to clarify the mechanisms of CDC in H2Mab-250.

Trastuzumab exerts antitumor activity through multiple mechanisms of action but is incapable of eliciting CDC in HER2-positive cancers in the presence of human serum [39,40]. As shown in Figure 1B, trastuzumab did not elicit CDC against BT-474 cells. An anti-HER2 bispecific and biparatopic antibody, zanidatamab, elicited potent CDC against HER2-high tumor cells, including BT-474 cells. Zanidatamab possesses an anti-HER2-ECD4 single chain variable fragment (scFv) linked to heavy chain 1 and an anti-HER2-ECD2 fragment antigen-binding (Fab) domain on heavy chain 2. Zanidatamab binds adjacent HER2 molecules in trans and initiates distinct HER2 reorganization and large HER2 clusters, not observed with trastuzumab [41]. Optimal CDC activity requires hexameric clustering of mAb Fc domains in the mAb-antigen clusters [42]. We identified the epitope of H2Mab-250 as 613-IWKFP-617 in the HER2-ECD4. The epitope of trastuzumab is a broader sequence (residues 579-625), which includes the H2Mab-250 epitope [33]. It is worthwhile to investigate the ability of H2Mab-250 to form the cluster with HER2.

The chimeric antigen receptor (CAR)-T cell therapy is rapidly advancing as cancer treatment; however, designing an optimal CAR remains challenging. Due to the specific reactivity against cancer cells, H2Mab-250 is clinically developed as CAR-T cell therapy, which is evaluated in a phase I study

Preprints.org (www.preprints.org) | NOT PEER-REVIEWED | Posted: 11 July 2024 doi:10.20944/preprints202407.0864.v1

for HER2-positive advanced solid tumors in the US (NCT06241456). We discussed the benefit of reducing CAR affinity to limit trogocytosis, which is observed in the high affinity of CAR-T cells [34]. In the monotherapy of H2Mab-250, we have reported compatible antitumor effects against breast cancer xenograft compared to trastuzumab [32,34] and showed the importance of CDC in this study. Extensive research indicates that resistance to CDC is induced by the expression of complement regulators in tumor cells during the escape from host immune responses. Notably, an upregulation of the regulators, including CD46, CD55, and CD59, has been shown to prevent CDC through suppression of terminal complement activation and MAC assembly [43–45]. In this regard, several strategies have been developed to overcome the resistance to CDC in mAb-based immunotherapy [46–49]. Therefore, dual targeting of HER2 by H2Mab-250 and complement regulators should be investigated in future studies in *in vitro* models.

4. Materials and Methods

4.1. Cell Culture

BT-474, SK-BR-3, and Chinese hamster ovary (CHO)-K1 were obtained from the American Type Culture Collection (ATCC, Manassas, VA). CHO-K1 and HER2-overexpressed CHO-K1 (CHO/HER2) were previously established [33] and were cultured in Roswell Park Memorial Institute (RPMI)-1640 medium (Nacalai Tesque, Inc., Kyoto, Japan). BT-474 and SK-BR-3 were cultured in Dulbecco's Modified Eagle Medium (DMEM) (Nacalai Tesque, Inc.). These were supplemented with 10% heat-inactivated fetal bovine serum (FBS; Thermo Fisher Scientific Inc.), 100 units/mL of penicillin, 100 μg/mL streptomycin, and 0.25 μg/mL amphotericin B (Nacalai Tesque, Inc.). All cell lines were cultured at 37°C in a humidified atmosphere with 5% CO_2 and 95% air.

4.2. Production of Recombinant mAbs

To generate a mouse-human chimeric mAb (H2Mab-250-hG1), V_H of H2Mab-250 and C_H of human IgG1 were cloned into the pCAG-Ble vector (FUJIFILM Wako Pure Chemical Corporation, Osaka, Japan). The V_L of H2Mab-250 and C_L of the human kappa light chain were cloned into the pCAG-Neo vector (FUJIFILM Wako Pure Chemical Corporation).

To generate mouse IgG2a-type H2Mab-250 (H2Mab-250-mG2a), we cloned the V_H cDNA of H2Mab-250 and C_H of mouse IgG2a into the pCAG-Ble vector. The mouse kappa light chain vector of H2Mab-250 was described above. To generate a mouse IgG2a type of trastuzumab (tras-mG2a), the V_H cDNA of trastuzumab and the C_H cDNA of mouse IgG2a were cloned into the pCAG-Neo vector, and the V_L cDNA of trastuzumab and the C_L cDNA of mouse kappa light chain were cloned into the pCAG-Ble vector.

To generate the recombinant PMab-231 for control mouse IgG2a, we cloned heavy and light chains of PMab-231 [50] into the pCAG-Neo and pCAG-Ble vectors, respectively.

The vectors were transfected into BINDS-09 (fucosyltransferase 8-knockout ExpiCHO-S) cells using the ExpiCHO Expression System (Thermo Fisher Scientific, Inc.) to produce the defucosylated mAbs. H2Mab-250-mG2a, tras-mG2a, H2Mab-250-hG1, trastuzumab, and PMab-231 were purified using Ab-Capcher (Kagawa, Japan). After washing with PBS, bound antibodies were eluted with an IgG elution buffer (Thermo Fisher Scientific Inc.) and immediately neutralized using 1M Tris-HCl (pH 8.0). Finally, the eluates were concentrated using Amicon Ultra (Merck KGaA) and replaced with PBS. The purified mAbs were confirmed by SDS-PAGE in reduced and non-reduced conditions (Supplementary Figure S3).

Normal human IgG was purchased from Sigma-Aldrich Corp. (St. Louis, MO).

4.3. ADCC

The ADCC of H2Mab-250-hG1 and trastuzumab was measured as follows. Human NK cells were purchased from Takara Bio, Inc. (Shiga, Japan) and were used as effector cells. The NK cells were used in the following experiment immediately after thawing. We labeled target cells (BT-474, SK-BR-3, CHO-K1, and CHO/HER2) using 10 μg/mL Calcein AM (Thermo Fisher Scientific, Inc.). The target cells were plated in 96-well plates (1×10^4 cells/well) and mixed with the human NK cells (effector to

Preprints.org (www.preprints.org) | NOT PEER-REVIEWED | Posted: 11 July 2024 doi:10.20944/preprints202407.0864.v1

target ratio, 50 : 1) and 100 μg/mL of H_2Mab-250-hG_1, trastuzumab or control human IgG. The calcein release was measured after a 4.5 h incubation. Fluorescence intensity was determined using a microplate reader (Power Scan HT; BioTek Instruments, Winooski, VT). After lysing all cells with a buffer containing 0.5% Triton X-100, 10 mM Tris-HCl (pH 7.4), and 10 mM EDTA, cytotoxicity (% lysis) was calculated as % lysis = (E − S)/(M − S) × 100, where E is the fluorescence of the combined target and effector cells, S is the spontaneous fluorescence of target cells only, and M is the maximum fluorescence measured.

The ADCC of H_2Mab-250-mG_{2a} and tras-mG_{2a} was measured as follows. Effector cells were obtained from the spleen of female BALB/c nude mice (Jackson Laboratory Japan, Inc., Kanagawa, Japan). The Calcein AM-labeled target cells (CHO-K1 and CHO/HER2) using 10 μg/mL Calcein AM were plated in 96-well plates (1×10^4 cells/well) and mixed with the effector cells (effector to target ratio, 50 : 1) with 100 μg/ml of H_2Mab-250-mG_{2a} and tras-mG_{2a} or control mouse IgG_{2a}. After a 4-hour incubation at 37°C, the Calcein release into the medium was measured, and the cytotoxicity (% lysis) was calculated as described above.

4.4. CDC

The calcein-labeled target cells (BT-474, SK-BR-3, CHO-K1, and CHO/HER2) were plated and mixed with rabbit complement (final dilution 1:10, or 1:15 [Fig. 2E], Low-Tox-M Rabbit Complement; Cedarlane Laboratories, Hornby, ON, Canada) and the indicated concentration of H_2Mab-250-hG_1, trastuzumab or control human IgG. Following incubation for 4.5 h at 37 °C, the calcein released into the medium was measured, as described above. In the case of H_2Mab-250-mG_{2a} and tras-mG_{2a} or control mouse IgG_{2a}, we performed a 4-hour incubation at 37°C. The cytotoxicity (% lysis) was calculated as described above.

4.5. Antitumor Activities of H_2Mab-250-hG_1, Trastuzumab, H_2Mab-250-mG_{2a}, and tras-mG_{2a}, in Tumor Xenograft Models

To examine the antitumor effect of H_2Mab-250-hG_1, trastuzumab, H_2Mab-250-mG_{2a}, and tras-mG_{2a}, animal experiments were approved by the Institutional Committee for Experiments of the Institute of Microbial Chemistry (approval no. 2023-066 and 2023-074). We monitored mice in a pathogen-free environment during the experimental period on an 11 h light/13 h dark cycle with food and water supplied ad libitum. Mice were monitored for health and weight every one or five days. We identified body weight loss exceeding 25% and maximum tumor size exceeding 3000 mm^3 as humane endpoints and terminated the experiments.

CHO/HER2 cells were suspended in 0.3 mL of 1.33×10^8 cells/mL using DMEM and mixed with 0.5 mL of BD Matrigel Matrix Growth Factor Reduced (BD Biosciences, San Jose, CA). Then, BALB/c nude mice (Jackson Laboratory Japan) were injected subcutaneously in the left flank with 100 μL of the suspension (5×10^6 cells). On day 9 post-inoculation, 100 μg of H_2Mab-250-mG_{2a} (n=8), tras-mG_{2a} (n=8), or control mouse IgG_{2a} (PMab-231; n = 8) in 100 μL PBS were intraperitoneally injected. On day 16, additional antibody injections were performed. The tumor diameter was measured on days 9, 16, and 21 after the inoculation of cells.

For evaluation of H_2Mab-250-hG_1 and trastuzumab, we injected the mice with 100 μg of H_2Mab-250-hG_1 (n = 8), trastuzumab (n = 8), or control human IgG (n = 8) in 100 μL of PBS through intraperitoneal injection on day 7 post-inoculation. Additional antibodies were injected on days 14 and 21. Furthermore, human NK cells (8.0×10^5 cells, Takara Bio, Inc.) were injected near the tumors subcutaneously on days 7, 14, and 21. The tumor diameter was measured on days 7, 14, 21, and 28 after inoculation with cells.

The tumor volume was calculated using the following formula: volume = $W^2 \times L/2$, where W is the short diameter and L is the long diameter. All mice were euthanized by cervical dislocation.

Statistical analyses were performed using GraphPad PRISM 6 (GraphPad Software, Inc., La Jolla, CA).

Preprints.org (www.preprints.org) | NOT PEER-REVIEWED | Posted: 11 July 2024 doi:10.20944/preprints202407.0864.v1

4.6. Pharmacokinetics of H_2Mab-250-hG_1 and Trastuzumab

HER2 ectodomain [34] was immobilized on Nunc Maxisorp 96−well immunoplates (Thermo Fisher Scientific Inc.) at a concentration of 1 μg/mL for 30 min at 37°C. After washing with PBS containing 0.05% (*v*/*v*) Tween 20 (PBST; Nacalai Tesque, Inc.), wells were blocked with 1% (*w*/*v*) bovine serum albumin (BSA)−containing PBST for 30 min at 37°C. To make a standard curve, the serially diluted H_2Mab-250-hG_1 and trastuzumab (0.00064–10 μg/mL) were added to each well, followed by peroxidase−conjugated anti−human Fc (1:3000 diluted; Sigma-Aldrich Corp.). Enzymatic reactions were conducted using ELISA POD Substrate TMB Kit (Nacalai Tesque, Inc.) followed by the measurement of the optical density at 655 nm, using an iMark microplate reader (Bio−Rad Laboratories, Inc., Berkeley, CA, USA). The standard curve was made using GraphPad PRISM 6. H_2Mab-250-hG_1 and trastuzumab (100 μg/mouse, n=3) were intraperitoneally injected and the serums were collected from day 0 (4 hours after injection) to 10. The concentration of mAbs was determined as described above. The half-life of mAbs was calculated as described previously [51].

Supplementary Materials: The following supporting information can be downloaded at the website of this paper posted on Preprints.org.

Author Contributions: H.S., T.O., and T.T. performed the experiments. M.K.K. and Y.K. designed the experiments. H.S., T.T., and Y.K. analyzed the data. H.S. and Y.K. wrote the manuscript. All authors have read and agreed to the published version of the manuscript.

Funding: This research was supported in part by Japan Agency for Medical Research and Development (AMED) under Grant Numbers: JP23ama121008 (to Y.K.), JP23am0401013 (to Y.K.), JP23bm1123027 (to Y.K.), JP23ck0106730 (to Y.K.), JP18am0301010 (to Y.K.), and JP21am0101078 (to Y.K.).

Institutional Review Board Statement: The Institutional Committee for Experiments of the Institute of Microbial Chemistry approved the animal experiment to examine the antitumor effect (approval no. 2023-066 and 2023-074).

Informed Consent Statement: Not applicable.

Data Availability Statement: The data presented in this study are available in the article.

Conflicts of Interest: The authors declare no conflict of interest.

References

1. Yarden, Y.; Sliwkowski, M.X. Untangling the ErbB signalling network. *Nat Rev Mol Cell Biol* **2001**, *2*, 127-137, doi:10.1038/35052073.
2. Slamon, D.J.; Clark, G.M.; Wong, S.G.; Levin, W.J.; Ullrich, A.; McGuire, W.L. Human breast cancer: correlation of relapse and survival with amplification of the HER-2/neu oncogene. *Science* **1987**, *235*, 177-182, doi:10.1126/science.3798106.
3. Van Cutsem, E.; Bang, Y.J.; Feng-Yi, F.; Xu, J.M.; Lee, K.W.; Jiao, S.C.; Chong, J.L.; López-Sanchez, R.I.; Price, T.; Gladkov, O.; et al. HER2 screening data from ToGA: targeting HER2 in gastric and gastroesophageal junction cancer. *Gastric Cancer* **2015**, *18*, 476-484, doi:10.1007/s10120-014-0402-y.
4. Tsao, L.C.; Force, J.; Hartman, Z.C. Mechanisms of Therapeutic Antitumor Monoclonal Antibodies. *Cancer Res* **2021**, *81*, 4641-4651, doi:10.1158/0008-5472.Can-21-1109.
5. Gschwind, A.; Fischer, O.M.; Ullrich, A. The discovery of receptor tyrosine kinases: targets for cancer therapy. *Nat Rev Cancer* **2004**, *4*, 361-370, doi:10.1038/nrc1360.
6. Slamon, D.J.; Leyland-Jones, B.; Shak, S.; Fuchs, H.; Paton, V.; Bajamonde, A.; Fleming, T.; Eiermann, W.; Wolter, J.; Pegram, M.; et al. Use of chemotherapy plus a monoclonal antibody against HER2 for metastatic breast cancer that overexpresses HER2. *N Engl J Med* **2001**, *344*, 783-792, doi:10.1056/nejm200103153441101.
7. Maadi, H.; Soheilifar, M.H.; Choi, W.S.; Moshtaghian, A.; Wang, Z. Trastuzumab Mechanism of Action; 20 Years of Research to Unravel a Dilemma. *Cancers (Basel)* **2021**, *13*, doi:10.3390/cancers13143540.
8. Cardoso, F.; Paluch-Shimon, S.; Senkus, E.; Curigliano, G.; Aapro, M.S.; André, F.; Barrios, C.H.; Bergh, J.; Bhattacharyya, G.S.; Biganzoli, L.; et al. 5th ESO-ESMO international consensus guidelines for advanced breast cancer (ABC 5). *Ann Oncol* **2020**, *31*, 1623-1649, doi:10.1016/j.annonc.2020.09.010.
9. Mark, C.; Lee, J.S.; Cui, X.; Yuan, Y. Antibody-Drug Conjugates in Breast Cancer: Current Status and Future Directions. *Int J Mol Sci* **2023**, *24*, doi:10.3390/ijms241813726.

Preprints.org (www.preprints.org) | NOT PEER-REVIEWED | Posted: 11 July 2024 doi:10.20944/preprints202407.0864.v1

10. Modi, S.; Saura, C.; Yamashita, T.; Park, Y.H.; Kim, S.B.; Tamura, K.; Andre, F.; Iwata, H.; Ito, Y.; Tsurutani, J.; et al. Trastuzumab Deruxtecan in Previously Treated HER2-Positive Breast Cancer. *N Engl J Med* **2020**, *382*, 610-621, doi:10.1056/NEJMoa1914510.
11. Shitara, K.; Bang, Y.J.; Iwasa, S.; Sugimoto, N.; Ryu, M.H.; Sakai, D.; Chung, H.C.; Kawakami, H.; Yabusaki, H.; Lee, J.; et al. Trastuzumab Deruxtecan in Previously Treated HER2-Positive Gastric Cancer. *N Engl J Med* **2020**, *382*, 2419-2430, doi:10.1056/NEJMoa2004413.
12. Modi, S.; Jacot, W.; Yamashita, T.; Sohn, J.; Vidal, M.; Tokunaga, E.; Tsurutani, J.; Ueno, N.T.; Prat, A.; Chae, Y.S.; et al. Trastuzumab Deruxtecan in Previously Treated HER2-Low Advanced Breast Cancer. *N Engl J Med* **2022**, *387*, 9-20, doi:10.1056/NEJMoa2203690.
13. Li, B.T.; Smit, E.F.; Goto, Y.; Nakagawa, K.; Udagawa, H.; Mazières, J.; Nagasaka, M.; Bazhenova, L.; Saltos, A.N.; Felip, E.; et al. Trastuzumab Deruxtecan in HER2-Mutant Non-Small-Cell Lung Cancer. *N Engl J Med* **2022**, *386*, 241-251, doi:10.1056/NEJMoa2112431.
14. Mercogliano, M.F.; Bruni, S.; Mauro, F.L.; Schillaci, R. Emerging Targeted Therapies for HER2-Positive Breast Cancer. *Cancers (Basel)* **2023**, *15*, doi:10.3390/cancers15071987.
15. Galvez-Cancino, F.; Simpson, A.P.; Costoya, C.; Matos, I.; Qian, D.; Peggs, K.S.; Litchfield, K.; Quezada, S.A. Fcγ receptors and immunomodulatory antibodies in cancer. *Nat Rev Cancer* **2024**, *24*, 51-71, doi:10.1038/s41568-023-00637-8.
16. Pereira, N.A.; Chan, K.F.; Lin, P.C.; Song, Z. The "less-is-more" in therapeutic antibodies: Afucosylated anti-cancer antibodies with enhanced antibody-dependent cellular cytotoxicity. *MAbs* **2018**, *10*, 693-711, doi:10.1080/19420862.2018.1466767.
17. Shinkawa, T.; Nakamura, K.; Yamane, N.; Shoji-Hosaka, E.; Kanda, Y.; Sakurada, M.; Uchida, K.; Anazawa, H.; Satoh, M.; Yamasaki, M.; et al. The absence of fucose but not the presence of galactose or bisecting N-acetylglucosamine of human IgG1 complex-type oligosaccharides shows the critical role of enhancing antibody-dependent cellular cytotoxicity. *J Biol Chem* **2003**, *278*, 3466-3473, doi:10.1074/jbc.M210665200.
18. Niwa, R.; Shoji-Hosaka, E.; Sakurada, M.; Shinkawa, T.; Uchida, K.; Nakamura, K.; Matsushima, K.; Ueda, R.; Hanai, N.; Shitara, K. Defucosylated chimeric anti-CC chemokine receptor 4 IgG1 with enhanced antibody-dependent cellular cytotoxicity shows potent therapeutic activity to T-cell leukemia and lymphoma. *Cancer Res* **2004**, *64*, 2127-2133, doi:10.1158/0008-5472.can-03-2068.
19. Yamane-Ohnuki, N.; Kinoshita, S.; Inoue-Urakubo, M.; Kusunoki, M.; Iida, S.; Nakano, R.; Wakitani, M.; Niwa, R.; Sakurada, M.; Uchida, K.; et al. Establishment of FUT8 knockout Chinese hamster ovary cells: an ideal host cell line for producing completely defucosylated antibodies with enhanced antibody-dependent cellular cytotoxicity. *Biotechnol Bioeng* **2004**, *87*, 614-622, doi:10.1002/bit.20151.
20. Golay, J.; Taylor, R.P. The Role of Complement in the Mechanism of Action of Therapeutic Anti-Cancer mAbs. *Antibodies (Basel)* **2020**, *9*, doi:10.3390/antib9040058.
21. Reis, E.S.; Mastellos, D.C.; Ricklin, D.; Mantovani, A.; Lambris, J.D. Complement in cancer: untangling an intricate relationship. *Nat Rev Immunol* **2018**, *18*, 5-18, doi:10.1038/nri.2017.97.
22. Taylor, R.P.; Lindorfer, M.A. Cytotoxic mechanisms of immunotherapy: Harnessing complement in the action of anti-tumor monoclonal antibodies. *Semin Immunol* **2016**, *28*, 309-316, doi:10.1016/j.smim.2016.03.003.
23. Reff, M.E.; Carner, K.; Chambers, K.S.; Chinn, P.C.; Leonard, J.E.; Raab, R.; Newman, R.A.; Hanna, N.; Anderson, D.R. Depletion of B cells in vivo by a chimeric mouse human monoclonal antibody to CD20. *Blood* **1994**, *83*, 435-445.
24. de Weers, M.; Tai, Y.T.; van der Veer, M.S.; Bakker, J.M.; Vink, T.; Jacobs, D.C.; Oomen, L.A.; Peipp, M.; Valerius, T.; Slootstra, J.W.; et al. Daratumumab, a novel therapeutic human CD38 monoclonal antibody, induces killing of multiple myeloma and other hematological tumors. *J Immunol* **2011**, *186*, 1840-1848, doi:10.4049/jimmunol.1003032.
25. Zent, C.S.; Secreto, C.R.; LaPlant, B.R.; Bone, N.D.; Call, T.G.; Shanafelt, T.D.; Jelinek, D.F.; Tschumper, R.C.; Kay, N.E. Direct and complement dependent cytotoxicity in CLL cells from patients with high-risk early-intermediate stage chronic lymphocytic leukemia (CLL) treated with alemtuzumab and rituximab. *Leuk Res* **2008**, *32*, 1849-1856, doi:10.1016/j.leukres.2008.05.014.
26. Schmudde, I.; Laumonnier, Y.; Köhl, J. Anaphylatoxins coordinate innate and adaptive immune responses in allergic asthma. *Semin Immunol* **2013**, *25*, 2-11, doi:10.1016/j.smim.2013.04.009.
27. Carroll, M.C.; Isenman, D.E. Regulation of humoral immunity by complement. *Immunity* **2012**, *37*, 199-207, doi:10.1016/j.immuni.2012.08.002.

Preprints.org (www.preprints.org) | NOT PEER-REVIEWED | Posted: 11 July 2024 doi:10.20944/preprints202407.0864.v1

28. Soares, L.R.; Vilbert, M.; Rosa, V.D.L.; Oliveira, J.L.; Deus, M.M.; Freitas-Junior, R. Incidence of interstitial lung disease and cardiotoxicity with trastuzumab deruxtecan in breast cancer patients: a systematic review and single-arm meta-analysis. *ESMO Open* **2023**, *8*, 101613, doi:10.1016/j.esmoop.2023.101613.
29. Copeland-Halperin, R.S.; Liu, J.E.; Yu, A.F. Cardiotoxicity of HER2-targeted therapies. *Curr Opin Cardiol* **2019**, *34*, 451-458, doi:10.1097/hco.0000000000000637.
30. Lee, K.F.; Simon, H.; Chen, H.; Bates, B.; Hung, M.C.; Hauser, C. Requirement for neuregulin receptor erbB2 in neural and cardiac development. *Nature* **1995**, *378*, 394-398, doi:10.1038/378394a0.
31. Crone, S.A.; Zhao, Y.Y.; Fan, L.; Gu, Y.; Minamisawa, S.; Liu, Y.; Peterson, K.L.; Chen, J.; Kahn, R.; Condorelli, G.; et al. ErbB2 is essential in the prevention of dilated cardiomyopathy. *Nat Med* **2002**, *8*, 459-465, doi:10.1038/nm0502-459.
32. Arimori, T.; Mihara, E.; Suzuki, H.; Ohishi, T.; Tanaka, T.; Kaneko, M.K.; Takagi, J.; Kato, Y. Locally misfolded HER2 expressed on cancer cells is a promising target for development of cancer-specific antibodies. *Structure* **2024**, doi:10.1016/j.str.2024.02.007.
33. Kaneko, M.K.; Suzuki, H.; Kato, Y. Establishment of a Novel Cancer-Specific Anti-HER2 Monoclonal Antibody H(2)Mab-250/H(2)CasMab-2 for Breast Cancers. *Monoclon Antib Immunodiagn Immunother* **2024**, *43*, 35-43, doi:10.1089/mab.2023.0033.
34. Kaneko, M.K.; Suzuki, H.; Ohishi, T.; Nakamura, T.; Tanaka, T.; Kato, Y. A Cancer-Specific Monoclonal Antibody against HER2 Exerts Antitumor Activities in Human Breast Cancer Xenograft Models. *Int J Mol Sci* **2024**, *25*, doi:10.3390/ijms25031941.
35. Suzuki, H.; Ohishi, T.; Tanaka, T.; Kaneko, M.K.; Kato, Y. A Cancer-Specific Monoclonal Antibody against Podocalyxin Exerted Antitumor Activities in Pancreatic Cancer Xenografts. *Int J Mol Sci* **2023**, *25*, doi:10.3390/ijms25010161.
36. Kato, Y.; Kaneko, M.K. A cancer-specific monoclonal antibody recognizes the aberrantly glycosylated podoplanin. *Sci Rep* **2014**, *4*, 5924, doi:10.1038/srep05924.
37. Yamada, S.; Ogasawara, S.; Kaneko, M.K.; Kato, Y. LpMab-23: A Cancer-Specific Monoclonal Antibody Against Human Podoplanin. *Monoclon Antib Immunodiagn Immunother* **2017**, *36*, 72-76, doi:10.1089/mab.2017.0001.
38. Merle, N.S.; Church, S.E.; Fremeaux-Bacchi, V.; Roumenina, L.T. Complement System Part I - Molecular Mechanisms of Activation and Regulation. *Front Immunol* **2015**, *6*, 262, doi:10.3389/fimmu.2015.00262.
39. Mamidi, S.; Cinci, M.; Hasmann, M.; Fehring, V.; Kirschfink, M. Lipoplex mediated silencing of membrane regulators (CD46, CD55 and CD59) enhances complement-dependent anti-tumor activity of trastuzumab and pertuzumab. *Mol Oncol* **2013**, *7*, 580-594, doi:10.1016/j.molonc.2013.02.011.
40. Wang, Y.; Yang, Y.J.; Wang, Z.; Liao, J.; Liu, M.; Zhong, X.R.; Zheng, H.; Wang, Y.P. CD55 and CD59 expression protects HER2-overexpressing breast cancer cells from trastuzumab-induced complement-dependent cytotoxicity. *Oncol Lett* **2017**, *14*, 2961-2969, doi:10.3892/ol.2017.6555.
41. Weisser, N.E.; Sanches, M.; Escobar-Cabrera, E.; O'Toole, J.; Whalen, E.; Chan, P.W.Y.; Wickman, G.; Abraham, L.; Choi, K.; Harbourne, B.; et al. An anti-HER2 biparatopic antibody that induces unique HER2 clustering and complement-dependent cytotoxicity. *Nat Commun* **2023**, *14*, 1394, doi:10.1038/s41467-023-37029-3.
42. Diebolder, C.A.; Beurskens, F.J.; de Jong, R.N.; Koning, R.I.; Strumane, K.; Lindorfer, M.A.; Voorhorst, M.; Ugurlar, D.; Rosati, S.; Heck, A.J.; et al. Complement is activated by IgG hexamers assembled at the cell surface. *Science* **2014**, *343*, 1260-1263, doi:10.1126/science.1248943.
43. Zipfel, P.F.; Skerka, C. Complement regulators and inhibitory proteins. *Nat Rev Immunol* **2009**, *9*, 729-740, doi:10.1038/nri2620.
44. Okroj, M.; Hsu, Y.F.; Ajona, D.; Pio, R.; Blom, A.M. Non-small cell lung cancer cells produce a functional set of complement factor I and its soluble cofactors. *Mol Immunol* **2008**, *45*, 169-179, doi:10.1016/j.molimm.2007.04.025.
45. Spiller, O.B.; Criado-García, O.; Rodríguez De Córdoba, S.; Morgan, B.P. Cytokine-mediated up-regulation of CD55 and CD59 protects human hepatoma cells from complement attack. *Clin Exp Immunol* **2000**, *121*, 234-241, doi:10.1046/j.1365-2249.2000.01305.x.
46. Sherbenou, D.W.; Aftab, B.T.; Su, Y.; Behrens, C.R.; Wiita, A.; Logan, A.C.; Acosta-Alvear, D.; Hann, B.C.; Walter, P.; Shuman, M.A.; et al. Antibody-drug conjugate targeting CD46 eliminates multiple myeloma cells. *J Clin Invest* **2016**, *126*, 4640-4653, doi:10.1172/jci85856.

Preprints.org (www.preprints.org) | NOT PEER-REVIEWED | Posted: 11 July 2024 doi:10.20944/preprints202407.0864.v1

47. Hu, W.; Ge, X.; You, T.; Xu, T.; Zhang, J.; Wu, G.; Peng, Z.; Chorev, M.; Aktas, B.H.; Halperin, J.A.; et al. Human CD59 inhibitor sensitizes rituximab-resistant lymphoma cells to complement-mediated cytolysis. *Cancer Res* **2011**, *71*, 2298-2307, doi:10.1158/0008-5472.Can-10-3016.
48. Geis, N.; Zell, S.; Rutz, R.; Li, W.; Giese, T.; Mamidi, S.; Schultz, S.; Kirschfink, M. Inhibition of membrane complement inhibitor expression (CD46, CD55, CD59) by siRNA sensitizes tumor cells to complement attack in vitro. *Curr Cancer Drug Targets* **2010**, *10*, 922-931, doi:10.2174/156800910793357952.
49. Imai, M.; Ohta, R.; Varela, J.C.; Song, H.; Tomlinson, S. Enhancement of antibody-dependent mechanisms of tumor cell lysis by a targeted activator of complement. *Cancer Res* **2007**, *67*, 9535-9541, doi:10.1158/0008-5472.Can-07-1690.
50. Furusawa, Y.; Kaneko, M.K.; Nakamura, T.; Itai, S.; Fukui, M.; Harada, H.; Yamada, S.; Kato, Y. Establishment of a Monoclonal Antibody PMab-231 for Tiger Podoplanin. *Monoclon Antib Immunodiagn Immunother* **2019**, *38*, 89-95, doi:10.1089/mab.2019.0003.
51. Rowland, M.; Tozer, T. Clinical pharmacokinetics and pharmacodynamics: concepts and applications (4th edition). Wolters Kluwer/Lippincott Williams & Wilkins: 2010.

Disclaimer/Publisher's Note: The statements, opinions and data contained in all publications are solely those of the individual author(s) and contributor(s) and not of MDPI and/or the editor(s). MDPI and/or the editor(s) disclaim responsibility for any injury to people or property resulting from any ideas, methods, instructions or products referred to in the content.